Published in final edited form as:
Neuron. 2015 February 4; 85(3): 519–533. doi:10.1016/j.neuron.2014.11.020.

IL-10 Alters Immunoproteostasis in *APP* mice, Increasing Plaque Burden and Worsening Cognitive Behavior

Paramita Chakrabarty[1,*], **Andrew Li**[1,#], **Carolina Ceballos-Diaz**[1], **James A. Eddy**[2], **Cory C Funk**[2], **Brenda Moore**[1], **Nadia DiNunno**[1], **Awilda M Rosario**[1], **Pedro E Cruz**[1], **Christophe Verbeeck**[3], **Amanda Sacino**[1], **Sarah Nix**[3], **Christopher Janus**[1], **Nathan D Price**[2], **Pritam Das**[3], and **Todd E Golde**[1,*]

[1]Department of Neuroscience, Center for Translational Research in Neurodegenerative Disease, McKnight Brain Institute, University of Florida, Gainesville, FL 32610, USA

[2]Institute for Systems Biology, 401 Terry Ave N, Seattle, WA 98109, USA

[3]Department of Neuroscience, Mayo Clinic College of Medicine, Jacksonville, FL 32224

Summary

Anti-inflammatory strategies are proposed to have beneficial effects in Alzheimer's disease. To explore how anti-inflammatory cytokine signaling affects Aβ pathology, we investigated the effects of adeno-associated virus (AAV2/1) mediated expression of Interleukin (IL)-10 in the brains of *APP* transgenic mouse models. IL-10 expression resulted in increased Aβ accumulation and impaired memory in *APP* mice. A focused transcriptome analysis revealed changes consistent with enhanced IL-10 signaling and increased ApoE expression in IL-10 expressing *APP* mice. ApoE protein was selectively increased in the plaque-associated insoluble cellular fraction, likely due to direct interaction with aggregated Aβ in the IL-10 expressing *APP* mice. *Ex vivo* studies also show that IL-10 and ApoE can individually impair glial Aβ phagocytosis. Our observations that IL-10 has an unexpected negative effect on Aβ proteostasis and cognition in *APP* mouse models demonstrate the complex interplay between innate immunity and proteostasis in neurodegenerative diseases, an interaction we call immunoproteostasis.

Introduction

Altered central nervous system (CNS) proteostasis, characterized by accumulation of extracellular or intracellular proteinaceous deposits, is thought to be a key trigger of many neurodegenerative disorders (Golde et al., 2013). There is considerable evidence that various assemblies of the aggregated proteins that form these inclusions can activate the innate immune system which, in turn, can contribute to the degenerative cascade. There is also

[*]Correspondence: tgolde@ufl.edu, pchakrabarty@ufl.edu.
[#]Present Address: Department of Biomedical Engineering, Johns Hopkins University, Baltimore, MD 21205, USA.

growing evidence that alterations in innate immune signaling can play a key role in regulating proteostasis of key pathogenic proteins linked to neurodegenerative disorders (reviewed in (Czirr and Wyss-Coray, 2012)). We term this complex interplay between the innate immune system and proteinopathy, immunoproteostasis. In a contextually dependent fashion, immunoproteostasis can have positive or negative effects on the proteinopathy and degenerative phenotype. Because of these effects and the plethora of therapeutic targets in the innate immune system, there is considerable interest in manipulating immunoproteostasis for potential disease modification in neurodegenerative diseases.

Two long-standing and interrelated hypotheses in the Alzheimer's disease (AD) field relevant to immunoproteostasis are that i) pro-inflammatory activation of innate immunity can enhance Aβ accumulation and thereby initiate or accelerate pathological cascades in AD and ii) anti-inflammatory strategies reduce Aβ accumulation and through synergistic or independent mechanisms could also be neuroprotective. We and others have directly tested the first of these hypotheses and found little experimental evidence to support it (Boissonneault et al., 2009; Chakrabarty et al., 2010b; Chakrabarty et al., 2011a; Chakrabarty et al., 2010a; El Khoury et al., 2007; Herber et al., 2007; Naert and Rivest, 2011; Shaftel et al., 2007). These studies showed that manipulations that skew innate immunity towards a pro-inflammatory state consistently reduce Aβ accumulation in transgenic mouse models largely by enhanced microglial clearance of Aβ. Other studies using pharmacologic and genetic means to suppress innate immune activation in similar mouse models have revealed conflicting results. Some manipulations designed to suppress innate immune activation appear to decrease Aβ accumulation and improve AD-associated phenotypes in these models, whereas others have deleterious effects and promote Aβ accumulation and worsen AD phenotypes (Chakrabarty et al., 2012; El Khoury et al., 2007; Kiyota et al., 2010; Maier et al., 2008; Richard et al., 2008; Vom Berg et al., 2012). Furthermore, clinical trials with anti-inflammatory agents have failed to clearly show any evidence of beneficial effect in AD patients (Breitner et al., 2011; Leoutsakos et al., 2012).

Given conflicting data on how suppressing immune activation can alter Aβ proteostasis, we explored the effects of Interleukin (IL)-10 expression in Amyloid Precursor protein (*APP*) transgenic mouse models. IL-10 is a key cytokine that represses excessive inflammatory responses and inhibits the effector functions in macrophages and myeloid cells by inhibiting inflammatory cytokine pathways (Banchereau et al., 2012). We tested the effect of recombinant adeno-associated virus (AAV2/1) mediated intracranial expression of murine IL-10 in two transgenic APP models: TgCRND8 (Chishti et al., 2001) and Tg2576 mice (Hsiao et al., 1995). We find that IL-10 expression leads to increased amyloid loads, decreased levels of immediate early genes and synaptic markers, worsened cognitive behavior, reduced microglial Aβ phagocytosis, increased ApoE expression and its sequestration within insoluble amyloid plaques.

Results

IL-10 exacerbates Aβ plaque burden in *APP* transgenic mice without affecting APP metabolism

We generated recombinant AAV vectors encoding murine *IL-10*. Transduction of HEK293T cells with the IL-10 expression construct showed that the IL-10 expressed from the AAV vector was efficiently secreted (Figure S1A). When primary neuroglial cultures were transduced with AAV2/1-*IL-10* and then subsequently treated with fibrillar Aβ42 (fAβ42) or LPS, IL-10 suppressed both fAβ42 and LPS induced inflammatory immune activation (Figure S1B).

We next evaluated the effects of IL-10 expression in two different *APP* mouse models. Two independent cohorts of neonatal transgenic TgCRND8 (Tg) mice and nontransgenic (nTg) littermates were injected with AAV2/1-*IL-10* or AAV2/1-*GFP* in the cerebral ventricles (ICV) and then analyzed after 5 or 6 months (Cohort A, Figure 1; Cohort B, Figure S2). We have previously shown that AAV2/1-*GFP* serves as an appropriate control for these types of studies (Chakrabarty et al., 2010b; Chakrabarty et al., 2010a). Following delivery of AAV2/1-*IL-10*, IL-10 was significantly increased in the brains and plasma of TgCRND8 (IL-10/Tg) and nTG (IL-10/nTg) mice (Figure S1, D-E). In the CRND8 Cohort A, analysis of Aβ plaque burden showed that IL-10 significantly increased total plaque burden by greater than 50% in the hippocampus and cortex of CRND8 mice while Thioflavin S (ThioS) positive dense core compact plaques increased by ∼38% (Figure 1A, B). Biochemical analysis of Aβ levels in sequentially extracted RIPA, SDS and formic acid (FA) solubilized mice brain lysates showed significantly increased levels of SDS solubilized Aβ and FA solubilized Aβ in IL-10/Tg mice (Figure 1C). There was no change in RIPA soluble Aβ (Figure 1C). Both the RIPA soluble and SDS soluble mouse brain extracts were separated by PAGE and examined using the Aβ N-terminus specific 82E1 monoclonal antibody. Levels of 82E1-immunoreactive low-molecular weight RIPA solubilized Aβ oligomers were unchanged in IL-10/Tg and control/Tg mice (data not shown). In the SDS fraction, an 82E1 immunoreactive band migrating at ∼8 kDa was slightly increased in a select group of IL-10/Tg mice (asterisk, Figure 1D). Immunofluorescence analysis of Aβ in microglia surrounding plaques showed increased Aβ accumulation within microglial cells in IL-10/Tg mice (Figure 1E). Notably, in the second cohort of CRND8 mice tested, we observed similar results on Aβ (Figure S2). We further tested whether accumulated Aβ in IL-10 expressing mice lead to increased phosphorylated tau. However, we found no significant changes in endogenous mouse tau phosphorylation in IL-10/Tg mice compared to Control/Tg mice (Figure S3).

We next examined whether IL-10 affects plaque deposition in another *APP* transgenic mouse model in a different experimental paradigm. 8-month old Tg2576 mice were injected in the hippocampus with AAV2/1-*IL-10* or AAV2/1-*GFP* and analyzed at 13 months of age. Soluble IL-10 was elevated in the brains of AAV2/1-*IL-10* injected mice (14.2±4.7ng/ml; 4.3× over control). Immunohistochemical analysis of Aβ plaque burden showed an overall increase of 43% in the brains of IL-10 expressing Tg2576 compared to GFP expressing mice without any change in Thioflavin S positive plaques (Figure 2A, B). ELISA analysis of Aβ

showed increased GN-HCl extractable insoluble Aβ42 but no changes in Aβ40 levels and unchanged levels of TBSx soluble Aβ (Figure 2C).

We performed an initial series of studies to evaluate IL-10 induced changes in *APP* gene expression, its cleavage products or Aβ degrading enzymes. No significant changes in full length APP, CTFα, CTFβ or PrPc were noted in CRND8 and Tg2576 cohorts (Figure S4A, C, D, E). Endogenous mouse APP and Aβ levels were not altered in nTg mice expressing IL-10 or GFP (Figure S4B, C, F). Q-RT-PCR of mouse APP, BACE1, IDE and human APP transcript levels did not reveal any significant alterations in IL-10 expressing mice (Figure S4G). Although NEP mRNA appeared to be lowered in IL-10/Tg mice (Figure S4G), NEP protein levels were not altered (Figure S4H).

IL-10 exacerbates context and fear tone memory in TgCRND8 mice

We assessed hippocampus-dependent contextual and amygdala-dependent tone fear conditioned (FC) memory in CRND8 mice (cohort A) (Figure 3A) (Hanna et al., 2012). All mice actively explored the novel environment of the training chamber and spent <3% of the total exploration time on pauses or immobility, with no significant differences between the groups (Figure 3B). The immediate freezing response to the foot shock significantly differentiated the groups, and was lower in both IL-10/Tg (13.6%) and Control/Tg (25.2%) mice as compared to IL-10/nTg (40.3%) and Control/nTg (34.9%) mice, respectively (Figure 3B). The freezing response of males and females was comparable, with no significant interactions involving gender ($p=0.377$, gender × group interaction effect). The IL-10/Tg mice showed decreased freezing during contextual memory test as compared to the control/nTg and control/Tg groups, which indicates the decline in their contextual fear memory (Figure 3C). Control/Tg mice showed comparable context memory to the memory of nTg mice (Figure 3C). During the tone test, the groups did not differ in their exploration of the modified chamber during the phase preceding the presentation of the tone (Figure 3D). IL-10/Tg mice froze significantly less than Control/nTg and IL-10/nTg mice during the presentation of the CS tone, while Control/Tg mice showed a trend of lower freezing response than Control/nTg mice (Figure 3D).

IL-10 reduces c-FOS and zif268 transcripts, and protein levels of synaptophysin and total PSD95

RNA analysis showed that IL-10/Tg mice displayed 62.8% reduction in the c-Fos transcript compared to Control/Tg mice (NanoString mouse inflammation GX array; log ratio=-1.315; $p=0.0250$; Q-value=0.00913). No significant change in c-fos transcript was detected in IL-10/nTg mice compared to Control/nTg mice. RNA levels of zif268, a key player in neuronal plasticity and learning, is also decreased in IL-10/Tg mice compared to Control/Tg mice (log ratio=-0.97; $p=0.00038$; Q-value=0.00029). We further examined levels of the presynaptic vesicle protein, synaptophysin, by immunohistochemistry and immunoblotting and found that IL-10/Tg mice have 27.5% less synaptophysin than Control/Tg (Figure 4A, B, C). In addition, though phospho-PSD95 protein is unchanged in IL-10/Tg, total levels of PSD95 are reduced by 50% in IL-10/Tg mice compared to control/Tg mice (Figure 4A, B).

IL-10 expression alters innate immune homeostasis in CRND8 mice and has modest effects on primary microglial phagocytosis

We investigated how IL-10 alters the immune milieu and Aβ phenotypes using i) immunophenotyping and immunohistochemical techniques and ii) functional assays to evaluate phagocytic potential of murine microglia and astrocytes. We analyzed how IL-10 affects the expression of M1 and M2 phenotypic markers in the CNS (Gordon and Taylor, 2005) (Figure 5A). Quantitative RT-PCR of IL-10/Tg or Control/Tg mice and their nTg littermates demonstrate a significant increase in Ym-1 in both IL-10/Tg and IL-10/nTg mice compared to genotype-matched control mice. MRC-1, Arginase or TGFβ transcript levels did not reach statistical significance. None of the M1-specific markers (IL-1β, IL-6, iNOS) showed significant alterations.

No gross morphological changes in the microglial or astrocyte processes were observed (Figure 5B). Immunoblotting with cd11b and GFAP showed a trend towards elevation in the IL-10/Tg mice (Figure 5C). Using either GFAP or Tomato lectin staining, we found that the number of astrocyte nuclei or microglial nuclei within a predefined area of 100 μm diameter around ThioS positive Aβ plaques were also unchanged (Figure 5D). Similar results were observed in the Tg2576 cohort injected with AAV2/1-*IL-10* (Figure S5).

Next we investigated the effect of recombinant IL-10 following fAβ42 treatment of primary murine microglial cells. In contrast to the broad immunosuppressive effect of IL-10 on mixed neuroglial cultures, IL-10 showed mixed effects on fAβ42 treated microglia. For example, IL-10 attenuated fAβ42 induced CCL5, CXCL10, TLR1 and TNFα expression but augmented CCL2 and CCL8 expression (Figure 6A). We then examined functional effects of IL-10 on the phagocytic potential of primary murine microglia and astrocytes cultured in vitro (Figure 6B, C; Figure S6). Wild type murine microglia or astrocytes were treated with recombinant cytokines, followed by addition of pre-aggregated fluorescent fAβ40 or fAβ42. Flow cytometric and microscopic analysis showed that IL-10 treatment leads to decreased internalized fAβ40 in IL-10 treated microglia compared to vehicle treated control microglia (Figure 6B, C). Following 1 hour of Aβ40 incubation, microglial cells were chased for 24 hours in fresh medium containing no Aβ. IL-10 treated cells showed a trend towards decreased clearance of internalized Aβ40 at 1 hour ($p=0.0533$, 1-tailed t-test) and 3 hour ($p=0.13$, 1-tailed t-test) following ‘chase’ in fresh medium (Figure S6A). Simultaneously, IL-6 treatment resulted in increased fAβ40 internalization compared to vehicle treated microglia after 1 hour incubation (Figure S6B). In these studies IL-10 did not affect fAβ42 uptake by microglia at the timepoints tested (Figure 6B). Astrocytes are relatively resistant to Aβ phagocytosis under similar experimental conditions (Chakrabarty et al., 2012). Flow cytometric analysis of fAβ40 or fAβ42 phagocytosis by murine astrocytes showed that IL-10 treatment does not alter Aβ internalization (Figure S6C) whereas IL-6 treatment leads to a significant increase in astrocytic Aβ internalization after 1 hour incubation (Figure S6B).

Integrated systems approach identifies inflammatory pathway changes in response to IL-10 expression in *APP* mice

We used NanoString gene expression arrays to perform expression profiling of RNAs that are altered by IL-10. Of the 179 mRNAs initially tested, 21 transcripts were significantly

altered, including chemokines and complement pathway genes (q-value < 0.05, Figure 7A). In a follow-up study, we constructed a Neurodegeneration custom array composed of key inflammatory and proteostasis mediators, including genes most up-regulated in the Inflammation GX array and other known mediators of neurodegenerative pathways (Table S1). Of the 240 genes tested in this array, we found that 140 genes were significantly differentially expressed in IL-10/Tg mice (99 up-regulated, 41 down-regulated, q-value < 0.05, Figure 7B, 7C, Table S2) and 47 genes were differentially expressed in IL-10/nTg mice (45 up-regulated, 2 down-regulated, q-value <0.05, Figure S7A, S7B, Table S3) compared to genotype matched controls. While the magnitude of change for common differentially expressed genes upon IL-10 expression is often greater in the nTg mice, the number of differentially expressed genes in Tg mice is significantly greater ($p < 0.0002$, two-tailed Z-test), indicating a more diverse effect of IL-10 in the Tg mice. Overall, the gene classes and pathway components altered most significantly in Tg and nTg mice were similar: chemokines (Tg:Ccl8, Ccl5; nTg:Ccl2, Ccl8), complements (Tg: C4a/4b, c3ar1, c1qb, c1qa; nTg: c1qa, C4a/4b, c1qb,), FcγRs (Tg: FcγR3a; nTg: FcγR2b) and immune signaling mediators (Tg: HLA-DRB1; nTg: Ly86, Ms4a6a, Ptpn6,Ctsc) (Figure 7C, S7B).

We used the Ingenuity Pathway Analysis (IPA) tool to identify biological pathways that are affected by over-expression of IL-10 in Tg and nTg mice. Differentially expressed genes were mapped to canonical pathways, which highlights individual immune and inflammatory signaling pathways that are most enriched for up- or down-regulated genes in both the Tg and nTg mice (Figure 7D, S7C; for a full list of altered pathways in Tg mice, see Table S4). Seven of the nine most significantly altered pathways we examined in the Tg mice included at least one directly overlapping gene with the IL-10 signaling pathway, supporting a role between IL-10 expression and downstream activation of these pathways. In the IL-10/Tg mice, pattern recognition and acute phase response pathways were the most significantly altered. In the IL-10/nTg mice, all the pathways affected have been classically defined as part of IL-10 signaling by multiple groups (Sabat, 2010; Shouval et al., 2014). We further applied the differential rank conservation (DIRAC) method to quantitatively measure how network expression ordering differs within and between phenotypes (Eddy et al., 2010); in this case, we included all measured genes in the analysis, as opposed to restricting the focus on differentially expressed genes as in IPA. Using DIRAC, we were able to identify multiple pathways in both Tg and nTg mice that were consistently reordered between IL-10 and control cohorts, such that these pathways could be used as statistically significant and accurate molecular classifiers (Figure 7E). Notably, the changes captured in these pathway signatures, especially among nTg mice, do not necessarily reflect pathway-level activation or repression in response to IL-10 overexpression, but often more subtle changes that manifest as relative changes in the expression levels of different components within a single pathway. In summary, we identified eight pathways that accurately distinguished between IL-10/Tg mice and control/Tg mice but were not significantly changed in nTg mice (100% of samples classified correctly by DIRAC) (Figure 7E; Table S5). The motivation of this study was not to develop classifiers; however, gene expression patterns within these pathways that accurately distinguish between IL-10 and control groups provide good measures of confidence for network-level differences. Moreover, these pathways represent

networks that are potentially altered in *APP* mice uniquely in response to IL-10 over-expression.

IL-10 increases ApoE expression and results in ApoE redistribution within amyloid plaque associated insoluble brain homogenate

Analysis of transcriptome changes in IL-10 expressing mice using NanoString array showed that IL-10 expression increased ApoE RNA levels in both Tg (↑1.7×, p=1.43E-06) and nTg (↑1.5×, p<0.05) mice (Table S2, S3). We observed a similar effect on ApoE transcription in AAV2/1-*IL-10* transduced primary mixed neuroglial cultures derived from wild type mice (Figure S8A). We did not find any significant changes in ApoE protein in sequentially extracted RIPA and SDS brain lysates of IL-10/Tg and Control/Tg mice (Figure 8A). However, increased levels of ApoE and cleavage products were found in the insoluble formic acid extracted IL-10/Tg mice brain lysates (↑3.87× compared to Control/TG, p<0.005), suggesting that IL-10 increases ApoE expression and alters its compartmentalization in Tg mice (Figure 8B). Immunofluorescence demonstrated that, as expected, ApoE was localized within astrocytes in both IL-10/Tg and Control/Tg mice (Figure S8B). In the IL-10/Tg mice ApoE immunostaining was also selectively increased within Aβ plaques, which is consistent with the increased ApoE sequestration in the formic acid biochemical fraction (Figure 8C, D).

To investigate whether ApoE can increase amyloidosis by directly affecting glial phagocytosis, we explored how ApoE conditioned media affects glial uptake of fluorescent Aβ. To recapitulate in vivo conditions, we transduced the astrocytes in mixed glial culture with either rAAV2/1-*GFP* or rAAV2/1-*ApoE* and maintained the mixed culture for 3 days (Figure S8C, D). Robust overexpression of ApoE was confirmed by Western blot analysis of conditioned media (Figure S8C). Microglia were then isolated from the mixed glial culture and phagocytosis of preformed fluorescent fAβ examined by immunofluorescence and flow cytometry. Microglial cells isolated from the ApoE treated culture and maintained in ApoE conditioned media showed a striking attenuation in internalization of fAβ compared to control microglia grown in GFP conditioned media (p=0.0027) (Figure 8E, S8D). Given the evidence for high affinity binding of ApoE to Aβ, we explored whether a direct interaction between Aβ aggregates and ApoE in the glial conditioned media might account for the dramatic effect on phagocytosis (Figure 8F). Pull-down assay using control aggregated amyloids (Iconomidou et al., 2001; Wilkins et al., 2000), aggregated Aβ42 and aggregated reverse Aβ42 showed that ApoE binds selectively to aggregated Aβ42 but not to the other amyloids (Figure 8F).

Discussion

In this study, we have directly tested the hypothesis that expression of the anti-inflammatory cytokine IL-10 would have beneficial effects in two *APP* mouse models. Rather than beneficial effects, we find that IL-10 worsens multiple AD relevant phenotypes in *APP* mice including amyloid plaque pathology and memory and learning. There was no evidence that the pro-amyloidogenic effect was due to altered *APP* expression or processing, nor were levels of key Aβ-degrading enzymes altered. IL-10 had a complex effect on innate immune

activation status in the brain. IL-10 altered the innate immune gene expression toward a M2-like activation state. Simultaneously, a network based approach identified several inflammatory pathways, consisting of chemokines and acute phase reactants, to be upregulated in IL-10 expressing Tg and nTg mice.

Mechanistically, we can attribute the negative effects of IL-10 on Aβ proteostasis to a synergistic effects of decreased Aβ phagocytosis by microglia, increased endogenous ApoE expression and enhanced accumulation of ApoE in insoluble amyloid plaques (summarized in Figure 8G). Our Aβ phagocytosis data, in combination with previous data with inflammatory cytokines (Chakrabarty et al., 2010a) indicates that IL-10 mediated alterations of innate immunity dampens microglial phagocytosis of Aβ in vitro. Additionally, ApoE by binding with Aβ aggregates, may negatively regulate Aβ aggregate clearance, thereby promoting further plaque deposition. Human APOE has been shown to have complex effects on Aβ. It promotes deposition of fibrillar Aβ, and in humans, can regulate clearance of soluble Aβ in an isoform dependent manner (reviewed in (Liu et al., 2013)). Human *APOE4* carriers are not only at risk for developing AD, but *APOE4* may also have negative impact on cognition in normal aging and AD (Corder et al., 1993; Deary et al., 2002; Honea et al., 2009; Liu et al., 2014). Mouse ApoE is comparable to human APOE4 at residues 112 and 158, and numerous studies suggest that the mouse protein may have enhanced amyloidogenic properties (Bales et al., 1997; DeMattos et al., 2004; Fagan et al., 2002; Holtzman et al., 2000a). Knocking out both endogenous mouse *ApoE* alleles reduces Aβ plaque deposition in *APP* mice (Holtzman et al., 2000a) and even haploinsufficiency reduces amyloid loads (Kim et al., 2011). Similarly, overexpression of APOE4 in pre-depositing *APP* mice exacerbates Aβ pathology whereas overexpression of APOE2 can enhance clearance of preexisting deposits (Dodart et al., 2005; Hudry et al., 2013). In our study, the increased level of insoluble ApoE is plaque-associated, consistent with mouse ApoE functioning as a pathological chaperone promoting Aβ fibrillogenesis (Bales et al., 1999; Holtzman et al., 1999; Holtzman et al., 2000b; Wisniewski et al., 1994). This is consistent with our immunofluorescence and amyloid pull down data that mouse ApoE preferentially associates with fibrillar Aβ, suggesting that the behavioral and amyloidogenic phenotype induced by IL-10 can result from the accumulation of Aβ bound to ApoE and possibly neurotoxic cleavage fragments ((Cho et al., 2001; Jones et al., 2011); reviewed in (Mahley and Huang, 2012)). However, it remains to be seen whether increasing the ‘protective’ forms of ApoE (ApoE2) can result in an opposite phenotype in the presence of IL-10, i.e., binding and clearing Aβ. Thus, this present study demonstrates that a key anti-inflammatory cytokine exacerbated Aβ proteostasis and brain function by altering Aβ clearance and/or deposition. These observations are highly consistent with unpublished data showing that *IL-10* deficiency in *APP* mice dramatically reduces Aβ load and other AD-related phenotypes, including lowered ApoE levels by RNAseq analysis (log_2FC=-0.6, FDR=4×10^-5) (M.-V. Guillot-Sestier and T. Town, personal communication).

This data is also highly consistent with our previous but relatively limited study, showing that direct intracranial expression of IL-4, another key anti-inflammatory cytokine, results in Aβ plaque accumulation in TgCRND8 mice (Chakrabarty et al., 2012). Furthermore, the data also agrees with our previously published findings that pro-inflammatory cytokines

(IL-6, TNF-α and IFN-γ) attenuated Aβ plaque deposition and increased microglial Aβ phagocytosis (Chakrabarty et al., 2010b; Chakrabarty et al., 2011a; Chakrabarty et al., 2010a). Thus, in contrast to the long-standing hypothesis that pro-inflammatory stimuli promote Aβ deposition, we find the opposite - anti-inflammatory stimuli promote amyloid deposition.

In two recent studies, AAV-mediated hippocampal targeted expression of IL-10 and IL-4 were reported to decrease gliosis and improve spatial memory in *APP/PS1* mice (Kiyota et al., 2012; Kiyota et al., 2010). Moreover, IL-4 but not IL-10, was reported to attenuate plaque deposition in these mice. Given that our IL-10 data was reproduced in two independent CRND8 cohorts and in a hippocampal paradigm in the Tg2576 mouse model, and a robust pro-amyloidogenic effect of IL-4 was observed both histochemically and confirmed biochemically in TgCRND8 mice (Chakrabarty et al., 2012), it is not easy to reconcile our observations with these previous reports. We would note that the group sizes in the Kiyota study are low, especially for behavioral analyses. Moreover, they do not specify gender of the mice, which can influence both behavioral effects and plaque loads in the bigenic *APP/PS1* mice (Wang et al., 2003). It is also possible the source of the discrepant observations could be attributed to the use of familial AD-linked mutant *PSEN1* transgenic mice, as PSEN1 has been reported to have immunomodulatory actions in the brain (Choi et al., 2008).

Although our own studies in this area have been internally consistent, a broader survey of published studies regarding alterations of Aβ and other phenotypes in *APP* mice via manipulation of chemokines, cytokines and other innate immune modulators suggests that a unified view of immunoproteostasis mechanisms in AD is not feasible at this time (Czirr and Wyss-Coray, 2012). Manipulations, such as LPS, TLR agonists or astrocytic overexpression of inflammatory cytokine IL-1β, that induce inflammatory glial activation reduce plaque load (Herber et al., 2007; Scholtzova et al., 2009; Shaftel et al., 2007). Thus, coupled with our previous observations in IL-6, IFN-γ and TNF- α overexpression paradigms in CRND8 mice (Chakrabarty et al., 2010b; Chakrabarty et al., 2011a; Chakrabarty et al., 2010a), these studies suggest that at least with respect to Aβ related phenotypes, a pro-inflammatory environment may have beneficial outcomes. However, other manipulations that can have an anti-inflammatory effect have also been shown to reduce plaques and improve cognition. Notable recent examples include genetic deficiency of inflammasome (*Nlrp3* or *Casp1* knockouts), deficiency of *Mrp14* and loss of IL-12/IL-23 signaling (Heneka et al., 2013; Vom Berg et al., 2012). Further additional manipulations, for example loss of *CD14, CD40L, Myd88,* fractalkine signaling, TGFβ signaling or overexpression of *TGFβ1* can have complex and sometimes unexpected effects on AD relevant phenotypes in mouse models that can be challenging to reconcile with data from similar paradigms (Lee et al., 2010; Lim et al., 2011; Reed-Geaghan et al., 2010; Tan et al., 1999; Town et al., 2008; Wyss-Coray et al., 2000).

Though genetic association studies have not reproducibly established the association of SNPs within the *IL-10* gene with AD risk, the recent and unequivocal associations of SNPs within other genetic loci that encode innate immunity genes bolster the preclinical data that innate immunity has a significant role in AD (Depboylu et al., 2003; Griciuc et al., 2013;

Guerreiro et al., 2013; Kamboh et al., 2012; Lambert et al., 2013). In spite of a clear contribution of immunoproteostasis in AD, epidemiologic and clinical data largely focused on NSAID use and AD risk, reveal a fairly conflicted literature related to anti-inflammatory strategies. Long-term NSAID use has been repeatedly shown to confer protection in epidemiologic studies (Szekely et al., 2004) but subsequent clinical trials with celecoxib and naproxen have not shown any benefits in patients (Martin et al., 2008). Given that select NSAIDs can modulate Aβ production, inhibit Aβ aggregation and affect other cell signaling pathways, it is possible that any potential protective effect of these NSAIDs could be due to target engagement other than cyclooxygenase (Lim et al., 2000; Weggen et al., 2001). A final intriguing observation relating to human NSAID use and AD is a report showing that naproxen use was associated with increased postmortem brain Aβ pathology (Sonnen et al., 2010). Though other pharmacologic approaches that might have anti-inflammatory effects (e.g., statins and PPARγ/α agonists) have been reported to have potential therapeutic benefit in AD preclinical models, to date none have shown efficacy in clinical trials nor has the effect in preclinical studies been unequivocally linked to effects on immunoproteostasis (Gold et al., 2010; Sano et al., 2011).

A striking feature of our study is the synergistic effect of IL-10 induced Aβ accumulation on fear conditioned memory and synaptic protein levels. As noted, IL-10 had minimal effect on learning and memory in the nTg littermates, but in the TgCRND8 transgenic mice, it significantly exacerbated context and tone fear memory, concurrent with marked loss of synaptic proteins. Although many studies suggest that soluble oligomeric species of Aβ are most often associated with various memory impairments in *APP* mice and humans (Zahs and Ashe, 2013), in TgCRND8 mice we have seen a strong correlation between total Aβ loads and impairments in fear conditioned memory (Hanna et al., 2012). Notably, multiple studies also show that increased insoluble APOE, both in humans and mice, is associated with worse cognitive function that is consistent with our observations (Bennett et al., 2005; Nilsson et al., 2004; Raber et al., 2000).

The observation that IL-10 can increase ApoE expression and promote its co-deposition with Aβ has implications for AD therapy. There is ample evidence that promoting expression of the protective APOE2 isoform would have beneficial effects and APOE4 harmful effects; thus, we might expect that increased IL-10 or any factor that promotes APOE expression in humans may have genotype dependent effects. Indeed, in the context of APOE2 one would propose that IL-10 could be beneficial if its effect on APOE is dominant. In contrast given the intermediate amyloid promoting effects of APOE3, empirical studies would be needed to determine effects of IL-10 in the context of APOE3.

In conclusion, we have demonstrated that IL-10 expression has a pro-amyloidogenic effect in *APP* mice leading to dysfunctional immunoproteostasis, impaired memory and reduction of synaptic markers. These data further highlight the complex role of innate immune activation in AD and other neurodegenerative diseases where specific innate manipulations can have unexpected positive or negative effects on proteostasis and neurodegeneration.

Experimental Procedures

Animal models and AAV2/1 injection

All animal procedures were approved by the Institutional Animal Care and Use Committee and done as previously described (Chakrabarty et al., 2010a). See Supplemental Experimental procedures for details.

Western blot, Immunohistochemistry, ELISA and RNA analysis

See Supplemental Experimental procedures for details.

Contextual Fear conditioning

See Supplemental Experimental procedures and Figure 3A for details.

Aβ Phagocytosis

Wild type murine microglia or astrocyte cultures were evaluated for uptake of fluorescently labeled fAβ42 or fAβ40 in the presence of cytokines. See Supplemental Experimental procedures for details.

RNA analysis

Transcriptome data obtained from NanoString array was analyzed using NanoStringNorm R, IPA and DIRAC as described in Supplemental Methods. Q-values were obtained as previously described (Storey and Tibshirani, 2003).

Statistical analysis

One-way or Two-way ANOVA with Tukey's multiple comparison test was used for statistical comparison unless otherwise stated (SigmaStat 3.0 version). For t-tests, multiple comparison test parameters were applied controlling for a false discovery rate of 5%. Graphical analyses were done using Prism 5 (GraphPad Software) and final images created using Photoshop CS2 (Adobe).

Supplementary Material

Refer to Web version on PubMed Central for supplementary material.

Acknowledgments

This work was supported by the Ellison Medical Foundation (TEG), NIH RO1AG32991 (PD) and NIH/NIA AG046139-01 (TEG, NP). We thank Drs. Terrence Town and Marie-Victoire Guillot-Sestier (University of Southern California) for helpful discussion.

References

Bales K, Verina T, Dodel R, Du Y, Altstiel L, Bender M, Hyslop P, Johnstone E, Little S, Cummins D, et al. Lack of apolipoprotein E dramatically reduces amyloid beta-peptide deposition. Nat Genet. 1997; 17:263–264. [PubMed: 9354781]

Bales KR, Verina T, Cummins DJ, Du Y, Dodel RC, Saura J, Fishman CE, DeLong CA, Piccardo P, Petegnief V, et al. Apolipoprotein E is essential for amyloid deposition in the APP(V717F)

transgenic mouse model of Alzheimer's disease. Proc Natl Acad Sci U S A. 1999; 96:15233–15238. [PubMed: 10611368]

Banchereau J, Pascual V, O'Garra A. From IL-2 to IL-37: the expanding spectrum of anti-inflammatory cytokines. Nat Immunol. 2012; 13:925–931. [PubMed: 22990890]

Bennett DA, Schneider JA, Wilson RS, Bienias JL, Berry-Kravis E, Arnold SE. Amyloid mediates the association of apolipoprotein E e4 allele to cognitive function in older people. Journal of neurology, neurosurgery, and psychiatry. 2005; 76:1194–1199.

Boissonneault V, Filali M, Lessard M, Relton J, Wong G, Rivest S. Powerful beneficial effects of macrophage colony-stimulating factor on beta-amyloid deposition and cognitive impairment in Alzheimer's disease. Brain. 2009; 132:1078–1092. [PubMed: 19151372]

Breitner JC, Baker LD, Montine TJ, Meinert CL, Lyketsos CG, Ashe KH, Brandt J, Craft S, Evans DE, Green RC, et al. Extended results of the Alzheimer's disease anti-inflammatory prevention trial. Alzheimers Dement. 2011; 7:402–411. [PubMed: 21784351]

Chakrabarty P, Ceballos-Diaz C, Beccard A, Janus C, Dickson D, Golde TE, Das P. IFN-gamma promotes complement expression and attenuates amyloid plaque deposition in amyloid beta precursor protein transgenic mice. J Immunol. 2010b; 184:5333–5343. [PubMed: 20368278]

Chakrabarty P, Herring A, Ceballos-Diaz C, Das P, Golde TE. Hippocampal expression of murine TNFalpha results in attenuation of amyloid deposition in vivo. Mol Neurodegener. 2011a; 6:16. [PubMed: 21324189]

Chakrabarty P, Jansen-West K, Beccard A, Ceballos-Diaz C, Levites Y, Verbeeck C, Zubair AC, Dickson D, Golde TE, Das P. Massive gliosis induced by interleukin-6 suppresses Abeta deposition in vivo: evidence against inflammation as a driving force for amyloid deposition. FASEB J. 2010a; 24:548–559. [PubMed: 19825975]

Chakrabarty P, Tianbai L, Herring A, Ceballos-Diaz C, Das P, Golde TE. Hippocampal expression of murine IL-4 results in exacerbation of amyloid deposition. Mol Neurodegener. 2012; 7:36. [PubMed: 22838967]

Chishti MA, Yang DS, Janus C, Phinney AL, Horne P, Pearson J, Strome R, Zuker N, Loukides J, French J, et al. Early-onset amyloid deposition and cognitive deficits in transgenic mice expressing a double mutant form of amyloid precursor protein 695. J Biol Chem. 2001; 276:21562–21570. [PubMed: 11279122]

Cho HS, Hyman BT, Greenberg SM, Rebeck GW. Quantitation of apoE domains in Alzheimer disease brain suggests a role for apoE in Abeta aggregation. J Neuropathol Exp Neurol. 2001; 60:342–349. [PubMed: 11305869]

Choi SH, Veeraraghavalu K, Lazarov O, Marler S, Ransohoff RM, Ramirez JM, Sisodia SS. Non-cell-autonomous effects of presenilin 1 variants on enrichment-mediated hippocampal progenitor cell proliferation and differentiation. Neuron. 2008; 59:568–580. [PubMed: 18760694]

Corder EH, Saunders AM, Strittmatter WJ, Schmechel DE, Gaskell PC, Small GW, Roses AD, Haines JL, Pericak-Vance MA. Gene dose of apolipoprotein E type 4 allele and the risk of Alzheimer's disease in late onset families. Science. 1993; 261:921–923. [PubMed: 8346443]

Czirr E, Wyss-Coray T. The immunology of neurodegeneration. J Clin Invest. 2012; 122:1156–1163. [PubMed: 22466657]

Deary IJ, Whiteman MC, Pattie A, Starr JM, Hayward C, Wright AF, Carothers A, Whalley LJ. Cognitive change and the APOE epsilon 4 allele. Nature. 2002; 418:932. [PubMed: 12198535]

DeMattos RB, Cirrito JR, Parsadanian M, May PC, O'Dell MA, Taylor JW, Harmony JA, Aronow BJ, Bales KR, Paul SM, et al. ApoE and clusterin cooperatively suppress Abeta levels and deposition: evidence that ApoE regulates extracellular Abeta metabolism in vivo. Neuron. 2004; 41:193–202. [PubMed: 14741101]

Depboylu C, Du Y, Muller U, Kurz A, Zimmer R, Riemenschneider M, Gasser T, Oertel WH, Klockgether T, Dodel RC. Lack of association of interleukin-10 promoter region polymorphisms with Alzheimer's disease. Neurosci Lett. 2003; 342:132–134. [PubMed: 12727335]

Dodart JC, Marr RA, Koistinaho M, Gregersen BM, Malkani S, Verma IM, Paul SM. Gene delivery of human apolipoprotein E alters brain Abeta burden in a mouse model of Alzheimer's disease. Proc Natl Acad Sci U S A. 2005; 102:1211–1216. [PubMed: 15657137]

Eddy JA, Hood L, Price ND, Geman D. Identifying tightly regulated and variably expressed networks by Differential Rank Conservation (DIRAC). PLoS computational biology. 2010; 6:e1000792. [PubMed: 20523739]

El Khoury J, Toft M, Hickman SE, Means TK, Terada K, Geula C, Luster AD. Ccr2 deficiency impairs microglial accumulation and accelerates progression of Alzheimer-like disease. Nat Med. 2007; 13:432–438. [PubMed: 17351623]

Fagan AM, Watson M, Parsadanian M, Bales KR, Paul SM, Holtzman DM. Human and murine ApoE markedly alters A beta metabolism before and after plaque formation in a mouse model of Alzheimer's disease. Neurobiol Dis. 2002; 9:305–318. [PubMed: 11950276]

Gold M, Alderton C, Zvartau-Hind M, Egginton S, Saunders AM, Irizarry M, Craft S, Landreth G, Linnamagi U, Sawchak S. Rosiglitazone monotherapy in mild-to-moderate Alzheimer's disease: results from a randomized, double-blind, placebo-controlled phase III study. Dement Geriatr Cogn Disord. 2010; 30:131–146. [PubMed: 20733306]

Golde TE, Borchelt DR, Giasson BI, Lewis J. Thinking laterally about neurodegenerative proteinopathies. J Clin Invest. 2013; 123:1847–1855. [PubMed: 23635781]

Gordon S, Taylor PR. Monocyte and macrophage heterogeneity. Nat Rev Immunol. 2005; 5:953–964. [PubMed: 16322748]

Griciuc A, Serrano-Pozo A, Parrado AR, Lesinski AN, Asselin CN, Mullin K, Hooli B, Choi SH, Hyman BT, Tanzi RE. Alzheimer's disease risk gene CD33 inhibits microglial uptake of amyloid beta. Neuron. 2013; 78:631–643. [PubMed: 23623698]

Guerreiro R, Wojtas A, Bras J, Carrasquillo M, Rogaeva E, Majounie E, Cruchaga C, Sassi C, Kauwe JS, Younkin S, et al. TREM2 variants in Alzheimer's disease. N Engl J Med. 2013; 368:117–127. [PubMed: 23150934]

Hanna A, Iremonger K, Das P, Dickson D, Golde T, Janus C. Age-related increase in amyloid plaque burden is associated with impairment in conditioned fear memory in CRND8 mouse model of amyloidosis. Alzheimers Res Ther. 2012; 4:21. [PubMed: 22697412]

Heneka MT, Kummer MP, Stutz A, Delekate A, Schwartz S, Vieira-Saecker A, Griep A, Axt D, Remus A, Tzeng TC, et al. NLRP3 is activated in Alzheimer's disease and contributes to pathology in APP/PS1 mice. Nature. 2013; 493:674–678. [PubMed: 23254930]

Herber DL, Mercer M, Roth LM, Symmonds K, Maloney J, Wilson N, Freeman MJ, Morgan D, Gordon MN. Microglial activation is required for Abeta clearance after intracranial injection of lipopolysaccharide in APP transgenic mice. J Neuroimmune Pharmacol. 2007; 2:222–231. [PubMed: 18040847]

Holtzman DM, Bales KR, Tenkova T, Fagan AM, Parsadanian M, Sartorius LJ, Mackey B, Olney J, McKeel D, Wozniak D, et al. Apolipoprotein E isoform-dependent amyloid deposition and neuritic degeneration in a mouse model of Alzheimer's disease. Proc Natl Acad Sci U S A. 2000a; 97:2892–2897. [PubMed: 10694577]

Holtzman DM, Bales KR, Wu S, Bhat P, Parsadanian M, Fagan AM, Chang LK, Sun Y, Paul SM. Expression of human apolipoprotein E reduces amyloid-beta deposition in a mouse model of Alzheimer's disease. J Clin Invest. 1999; 103:R15–R21. [PubMed: 10079115]

Holtzman DM, Fagan AM, Mackey B, Tenkova T, Sartorius L, Paul SM, Bales K, Ashe KH, Irizarry MC, Hyman BT. Apolipoprotein E facilitates neuritic and cerebrovascular plaque formation in an Alzheimer's disease model. Ann Neurol. 2000b; 47:739–747. [PubMed: 10852539]

Honea RA, Vidoni E, Harsha A, Burns JM. Impact of APOE on the healthy aging brain: a voxel-based MRI and DTI study. J Alzheimers Dis. 2009; 18:553–564. [PubMed: 19584447]

Hsiao KK, Borchelt DR, Olson K, Johannsdottir R, Kitt C, Yunis W, Xu S, Eckman C, Younkin S, Price D, et al. Age-related CNS disorder and early death in transgenic FVB/N mice overexpressing Alzheimer amyloid precursor proteins. Neuron. 1995; 15:1203–1218. [PubMed: 7576662]

Hudry E, Dashkoff J, Roe AD, Takeda S, Koffie RM, Hashimoto T, Scheel M, Spires-Jones T, Arbel-Ornath M, Betensky R, et al. Gene transfer of human Apoe isoforms results in differential modulation of amyloid deposition and neurotoxicity in mouse brain. Science translational medicine. 2013; 5:212ra161.

Iconomidou VA, Chryssikos GD, Gionis V, Vriend G, Hoenger A, Hamodrakas SJ. Amyloid-like fibrils from an 18-residue peptide analogue of a part of the central domain of the B-family of silkmoth chorion proteins. FEBS Lett. 2001; 499:268–273. [PubMed: 11423129]

Jones PB, Adams KW, Rozkalne A, Spires-Jones TL, Hshieh TT, Hashimoto T, von Armin CA, Mielke M, Bacskai BJ, Hyman BT. Apolipoprotein E: isoform specific differences in tertiary structure and interaction with amyloid-beta in human Alzheimer brain. PLoS One. 2011; 6:e14586. [PubMed: 21297948]

Kamboh MI, Demirci FY, Wang X, Minster RL, Carrasquillo MM, Pankratz VS, Younkin SG, Saykin AJ, Jun G, et al. Alzheimer's Disease Neuroimaging I. Genome-wide association study of Alzheimer's disease. Translational psychiatry. 2012; 2:e117. [PubMed: 22832961]

Kim J, Jiang H, Park S, Eltorai AE, Stewart FR, Yoon H, Basak JM, Finn MB, Holtzman DM. Haploinsufficiency of human APOE reduces amyloid deposition in a mouse model of amyloid-beta amyloidosis. J Neurosci. 2011; 31:18007–18012. [PubMed: 22159114]

Kiyota T, Ingraham KL, Swan RJ, Jacobsen MT, Andrews SJ, Ikezu T. AAV serotype 2/1-mediated gene delivery of anti-inflammatory interleukin-10 enhances neurogenesis and cognitive function in APP+PS1 mice. Gene Ther. 2012; 19:724–733. [PubMed: 21918553]

Kiyota T, Okuyama S, Swan RJ, Jacobsen MT, Gendelman HE, Ikezu T. CNS expression of anti-inflammatory cytokine interleukin-4 attenuates Alzheimer's disease-like pathogenesis in APP+PS1 bigenic mice. FASEB J. 2010; 24:3093–3102. [PubMed: 20371618]

Lambert JC, Ibrahim-Verbaas CA, Harold D, Naj AC, Sims R, Bellenguez C, DeStafano AL, Bis JC, Beecham GW, Granier-Boley B, et al. Meta-analysis of 74,046 individuals identifies 11 new susceptibility loci for Alzheimer's disease. Nat Genet. 2013; 45:1452–1458. [PubMed: 24162737]

Lee S, Varvel NH, Konerth ME, Xu G, Cardona AE, Ransohoff RM, Lamb BT. CX3CR1 deficiency alters microglial activation and reduces beta-amyloid deposition in two Alzheimer's disease mouse models. Am J Pathol. 2010; 177:2549–2562. [PubMed: 20864679]

Leoutsakos JM, Muthen BO, Breitner JC, Lyketsos CG. Effects of non-steroidal anti-inflammatory drug treatments on cognitive decline vary by phase of pre-clinical Alzheimer disease: findings from the randomized controlled Alzheimer's Disease Anti-inflammatory Prevention Trial. Int J Geriatr Psychiatry. 2012; 27:364–374. [PubMed: 21560159]

Lim GP, Yang F, Chu T, Chen P, Beech W, Teter B, Tran T, Ubeda O, Ashe KH, Frautschy SA, et al. Ibuprofen suppresses plaque pathology and inflammation in a mouse model for Alzheimer's disease. J Neurosci. 2000; 20:5709–5714. [PubMed: 10908610]

Lim JE, Kou J, Song M, Pattanayak A, Jin J, Lalonde R, Fukuchi K. MyD88 deficiency ameliorates beta-amyloidosis in an animal model of Alzheimer's disease. Am J Pathol. 2011; 179:1095–1103. [PubMed: 21763676]

Liu CC, Kanekiyo T, Xu H, Bu G. Apolipoprotein E and Alzheimer disease: risk, mechanisms and therapy. Nat Rev Neurol. 2013; 9:106–118. [PubMed: 23296339]

Liu Y, Yu JT, Wang HF, Han PR, Tan CC, Wang C, Meng XF, Risacher SL, Saykin AJ, Tan L. APOE genotype and neuroimaging markers of Alzheimer's disease: systematic review and meta-analysis. Journal of neurology, neurosurgery, and psychiatry. 2014

Mahley RW, Huang Y. Apolipoprotein e sets the stage: response to injury triggers neuropathology. Neuron. 2012; 76:871–885. [PubMed: 23217737]

Maier M, Peng Y, Jiang L, Seabrook TJ, Carroll MC, Lemere CA. Complement C3 deficiency leads to accelerated amyloid beta plaque deposition and neurodegeneration and modulation of the microglia/macrophage phenotype in amyloid precursor protein transgenic mice. J Neurosci. 2008; 28:6333–6341. [PubMed: 18562603]

Martin BK, Szekely C, Brandt J, Piantadosi S, Breitner JC, Craft S, Evans D, Green R, Mullan M. Cognitive function over time in the Alzheimer's Disease Anti-inflammatory Prevention Trial (ADAPT): results of a randomized, controlled trial of naproxen and celecoxib. Arch Neurol. 2008; 65:896–905. [PubMed: 18474729]

Naert G, Rivest S. CC chemokine receptor 2 deficiency aggravates cognitive impairments and amyloid pathology in a transgenic mouse model of Alzheimer's disease. J Neurosci. 2011; 31:6208–6220. [PubMed: 21508244]

Nilsson LN, Arendash GW, Leighty RE, Costa DA, Low MA, Garcia MF, Cracciolo JR, Rojiani A, Wu X, Bales KR, et al. Cognitive impairment in PDAPP mice depends on ApoE and ACT-catalyzed amyloid formation. Neurobiol Aging. 2004; 25:1153–1167. [PubMed: 15312961]

Raber J, Wong D, Yu GQ, Buttini M, Mahley RW, Pitas RE, Mucke L. Apolipoprotein E and cognitive performance. Nature. 2000; 404:352–354. [PubMed: 10746713]

Reed-Geaghan EG, Reed QW, Cramer PE, Landreth GE. Deletion of CD14 attenuates Alzheimer's disease pathology by influencing the brain's inflammatory milieu. J Neurosci. 2010; 30:15369–15373. [PubMed: 21084593]

Richard KL, Filali M, Prefontaine P, Rivest S. Toll-like receptor 2 acts as a natural innate immune receptor to clear amyloid beta 1-42 and delay the cognitive decline in a mouse model of Alzheimer's disease. J Neurosci. 2008; 28:5784–5793. [PubMed: 18509040]

Sabat R. IL-10 family of cytokines. Cytokine Growth Factor Rev. 2010; 21:315–324. [PubMed: 21112807]

Sano M, Bell KL, Galasko D, Galvin JE, Thomas RG, van Dyck CH, Aisen PS. A randomized, double-blind, placebo-controlled trial of simvastatin to treat Alzheimer disease. Neurology. 2011; 77:556–563. [PubMed: 21795660]

Scholtzova H, Kascsak RJ, Bates KA, Boutajangout A, Kerr DJ, Meeker HC, Mehta PD, Spinner DS, Wisniewski T. Induction of toll-like receptor 9 signaling as a method for ameliorating Alzheimer's disease-related pathology. J Neurosci. 2009; 29:1846–1854. [PubMed: 19211891]

Shaftel SS, Kyrkanides S, Olschowka JA, Miller JN, Johnson RE, O'Banion MK. Sustained hippocampal IL-1 beta overexpression mediates chronic neuroinflammation and ameliorates Alzheimer plaque pathology. J Clin Invest. 2007; 117:1595–1604. [PubMed: 17549256]

Shouval DS, Ouahed J, Biswas A, Goettel JA, Horwitz BH, Klein C, Muise AM, Snapper SB. Interleukin 10 receptor signaling: master regulator of intestinal mucosal homeostasis in mice and humans. Advances in immunology. 2014; 122:177–210. [PubMed: 24507158]

Sonnen JA, Larson EB, Walker RL, Haneuse S, Crane PK, Gray SL, Breitner JC, Montine TJ. Nonsteroidal anti-inflammatory drugs are associated with increased neuritic plaques. Neurology. 2010; 75:1203–1210. [PubMed: 20811000]

Storey JD, Tibshirani R. Statistical significance for genomewide studies. Proc Natl Acad Sci U S A. 2003; 100:9440–9445. [PubMed: 12883005]

Szekely CA, Thorne JE, Zandi PP, Ek M, Messias E, Breitner JC, Goodman SN. Nonsteroidal anti-inflammatory drugs for the prevention of Alzheimer's disease: a systematic review. Neuroepidemiology. 2004; 23:159–169. [PubMed: 15279021]

Tan J, Town T, Paris D, Mori T, Suo Z, Crawford F, Mattson MP, Flavell RA, Mullan M. Microglial activation resulting from CD40-CD40L interaction after beta- amyloid stimulation. Science. 1999; 286:2352–2355. [PubMed: 10600748]

Town T, Laouar Y, Pittenger C, Mori T, Szekely CA, Tan J, Duman RS, Flavell RA. Blocking TGF-beta-Smad2/3 innate immune signaling mitigates Alzheimer-like pathology. Nat Med. 2008; 14:681–687. [PubMed: 18516051]

Vom Berg J, Prokop S, Miller KR, Obst J, Kalin RE, Lopategui-Cabezas I, Wegner A, Mair F, Schipke CG, Peters O, et al. Inhibition of IL-12/IL-23 signaling reduces Alzheimer's disease-like pathology and cognitive decline. Nat Med. 2012; 18:1812–1819. [PubMed: 23178247]

Wang J, Tanila H, Puolivali J, Kadish I, van Groen T. Gender differences in the amount and deposition of amyloidbeta in APPswe and PS1 double transgenic mice. Neurobiol Dis. 2003; 14:318–327. [PubMed: 14678749]

Weggen S, Eriksen JL, Das P, Sagi SA, Wang R, Pietrzik CU, Findlay KA, Smith TE, Murphy MP, Bulter T, et al. A subset of NSAIDs lower amyloidogenic Abeta42 independently of cyclooxygenase activity. Nature. 2001; 414:212–216. [PubMed: 11700559]

Wilkins DK, Dobson CM, Gross M. Biophysical studies of the development of amyloid fibrils from a peptide fragment of cold shock protein B. Eur J Biochem. 2000; 267:2609–2616. [PubMed: 10785381]

Wisniewski T, Castano EM, Golabek A, Vogel T, Frangione B. Acceleration of Alzheimer's fibril formation by apolipoprotein E in vitro. American Journal of Pathology. 1994; 145:1030–1035. [PubMed: 7977635]

Wyss-Coray T, Lin C, Sanan DA, Mucke L, Masliah E. Chronic overproduction of transforming growth factor-beta1 by astrocytes promotes Alzheimer's disease-like microvascular degeneration in transgenic mice. Am J Pathol. 2000; 156:139–150. [PubMed: 10623661]

Zahs KR, Ashe KH. beta-Amyloid oligomers in aging and Alzheimer's disease. Front Aging Neurosci. 2013; 5:28. [PubMed: 23847532]

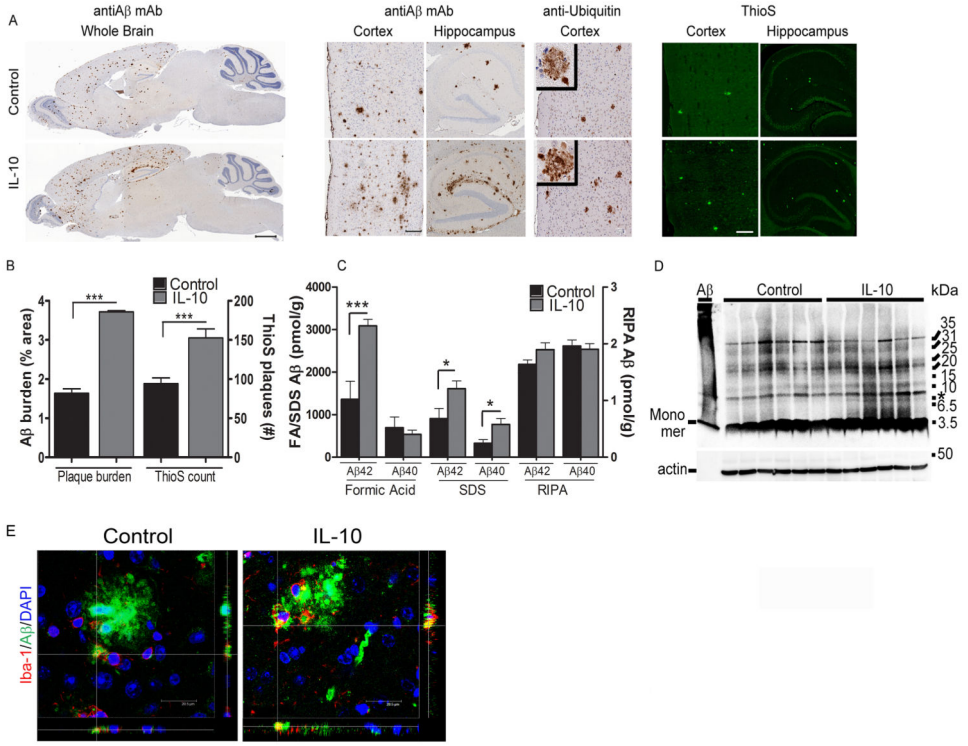

Figure 1. IL-10 increases Aβ deposition in Tg CRND8 mice

A. Neonatal CRND8 mice were injected with either AAV2/1-*IL-10* or AAV2/1-*GFP* (control) in the cerebral ventricles and analyzed after 6 months for Aβ plaque pathology using anti Aβ mAb 33.1.1, anti-ubiquitin and ThioS staining. Both Aβ staining protocols depict increased Aβ deposition in IL-10/Tg mice compared to controls whereas ubiquitin staining around individual plaques was unaltered. Scale Bar, 600μm (whole brain), 125μm (cortex and hippocampus). n=8-10mice/group for immunohistochemistry and n=6/group for ThioS staining.

B. Quantification of Aβ plaque shows significantly increased amyloid plaque burden (immunostained with anti Aβ 33.1.1) and total number of ThioS cored plaques in IL-10/Tg mice compared to control/Tg mice. Data represents mean ± sem. n=8-10/group for immunohistochemistry and n=6 mice/group for ThioS staining. ***p<0.001, unpaired two-tailed t test).

C. Biochemical analyses of sequentially extracted Aβ42 and Aβ40 levels by end-specific sandwich ELISA show significantly increased SDS soluble and formic acid extractable insoluble Aβ levels in IL-10/Tg compared to control/Tg mice. No change was detected in RIPA extracted Aβ42 and Aβ40. Data represents mean ± sem. n=6 mice/group. (*p<0.05, ***p<0.001, 2 way Anova with Tukey's multiple comparison test).

D. Representative 82E1 immunoblots of 6 month old IL-10/Tg mice show no significant changes in Aβ oligomers compared to control/Tg mice. The left lane shows a representative aggregated Aβ42 preparation. A band migrating ~8kDa is upregulated in select IL-10/Tg mice (asterisk, right). Molecular weight markers are indicated on the right (kDa). The lower panel represents the 82E1 blot re-probed with anti-actin antibody to depict loading amount. n=6 mice/group.

E. Representative Z slice section analysis of 4G8 immunoreactive Aβ (Alexa Fluor 488nm) and Iba-1 labeled microglia (Alexa Fluor 594nm) shows increased Aβ accumulation in microglia surrounding amyloid plaques in IL-10/Tg mice. DAPI, in blue, denotes nucleus. Scale bar, 20.5μm. n=3 mice/group. See also Figures S1-S4.

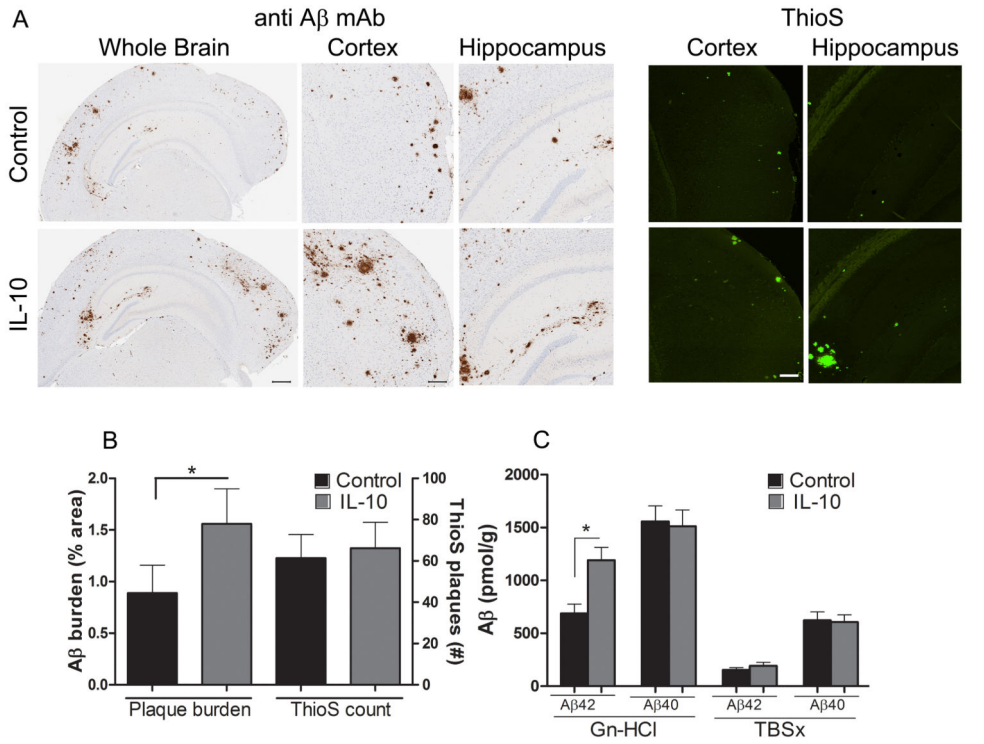

Figure 2. IL-10 increases Aβ deposition in Tg2576 mice

A.8 month old Tg2576 mice were injected in the hippocampus with AAV2/1-*IL-10* or AAV2/1-*GFP* (Control), aged for 5 months and analyzed at 13 months. Representative brain sections (cortex and hippocampus) stained with anti-Aβ mAb 33.1.1 show that Aβ plaque burden is increased in IL-10 expressing mice compared to control. No significant changes in ThioS stained cored plaques was observed. Scale Bar, 125μm (whole brain), 75μm (cortex and hippocampus). n=5-7 mice/group.

B. Quantitative burden analysis of Aβ plaque deposits show significantly increased Aβ plaque immunoreactivity but no change in ThioS reactive plaques in IL-10 expressing mice compared to controls. Data represents mean ± sem. n=5-7 mice/group. *p< 0.05, Unpaired t test.

C. Biochemical analyses of Gn-HCL solubilized Aβ42 and Aβ40 levels measured by ELISA show significantly increased insoluble Aβ42 levels in IL-10 expressing mice compared to controls but no significant differences in soluble Aβ levels (TBSx fraction) are seen. Data represents mean ± sem. n=5-7 mice/group. *p< 0.05, Unpaired t test. See also Figure S4.

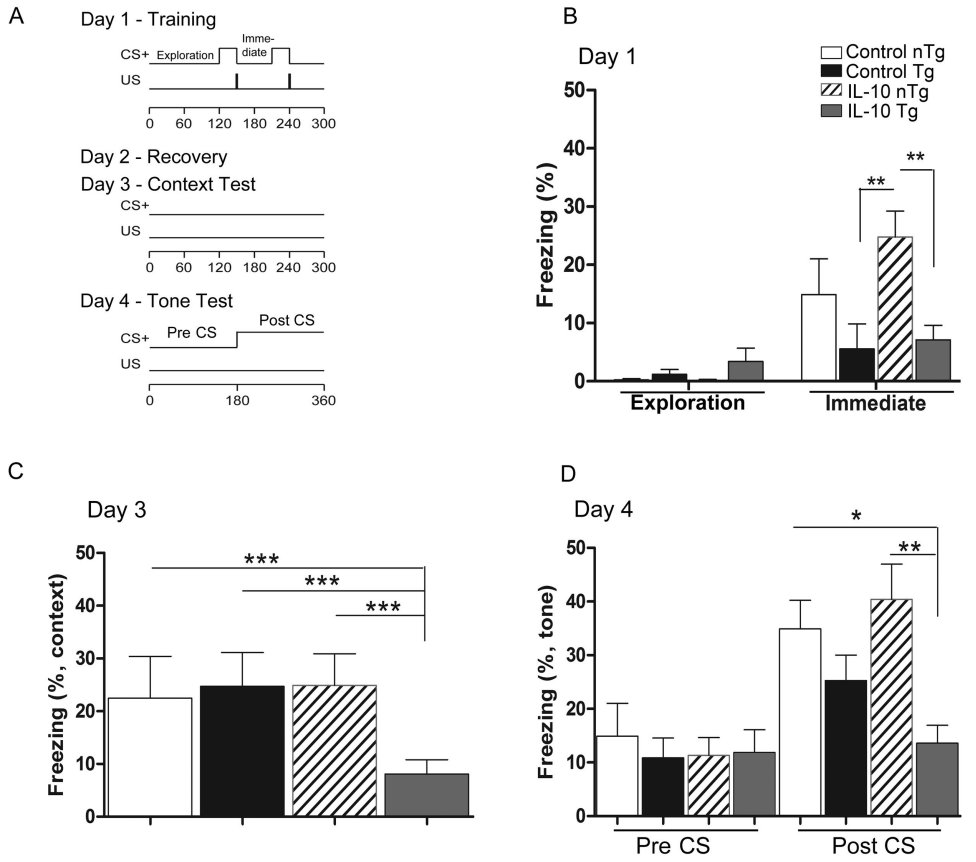

Figure 3. IL-10 worsens cognitive impairment in TgCRND8 mice

A. Schematic representation of the stimuli parameters used in delay conditioning paradigms. On day 1, mice were exposed to two pairings of an auditory conditioned stimulus (CS) and a brief co-terminating foot shock (US). After a day of recovery (day 2), the memory of the association between the training context and the US was evaluated on day 3, and the memory of the association between the tone CS and US evaluated on day 4.

B. Mean percent of freezing exhibited by IL-10 expressing and control groups during training. All mice showed comparable activity in the training chamber, pausing briefly during their exploration of the novel environment of the chamber before the onset of the first tone stimulus. The evaluation of freezing response immediately following the presentation of a foot shock during training showed that both the control/Tg and IL-10/Tg mice froze less as compared to control/nTg mice and IL-10/nTg mice respectively (n=8-12/group). **p < 0.01, MODLSD Bonferroni t-tests.

C-D. In the context test, IL-10/Tg mice showed significantly lower rates of freezing compared to control/Tg mice as well as nTg littermates expressing GFP or IL-10 indicative of severe memory deficits (**C**). During the tone test, there was no difference in the freezing response of the mice in the modified context of the chamber at the stage preceding tone presentation (Pre CS, D). During tone presentation (Post CS, D), IL-10/Tg mice showed significantly weaker tone fear memory as compared to their control/nTg and IL-10/Tg littermates, while the control/Tg mice showed a trend in freezing decrease as compared to

Control/nTg ($p=0.07$) (n=8-12 mice/group). *$p<0.05$, **$p < 0.01$, ***$p<0.001$, MODLSD Bonferroni t-tests.

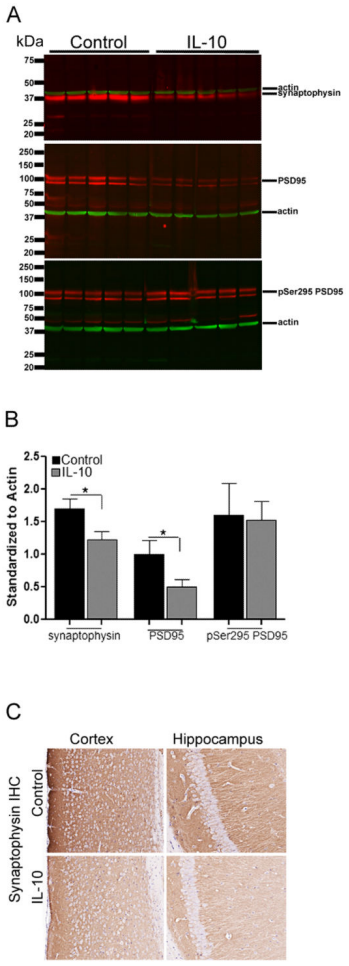

Figure 4. IL-10 induced cognitive impairment is accompanied by reduced synaptic proteins

A-B. Synaptophysin, PSD95 and phosphorylated PSD95 (pSer295 PSD95) levels in 6 month old IL-10/Tg and control/Tg mice. Molecular weight markers are indicated on the left (kDa). All blots were simultaneously reprobed with anti-actin antibody to depict loading amount. Intensity analysis (mean ± sem) of immunoreactive bands of interest were normalized to β-actin (B). n=5 mice/group; *p<0.05, Unpaired two-tailed t test.

C. Synaptophysin immunoreactivity was decreased in both the cortex and hippocampus of IL-10/Tg mice compared to control/Tg. Scale, 150μm, n=5/group.

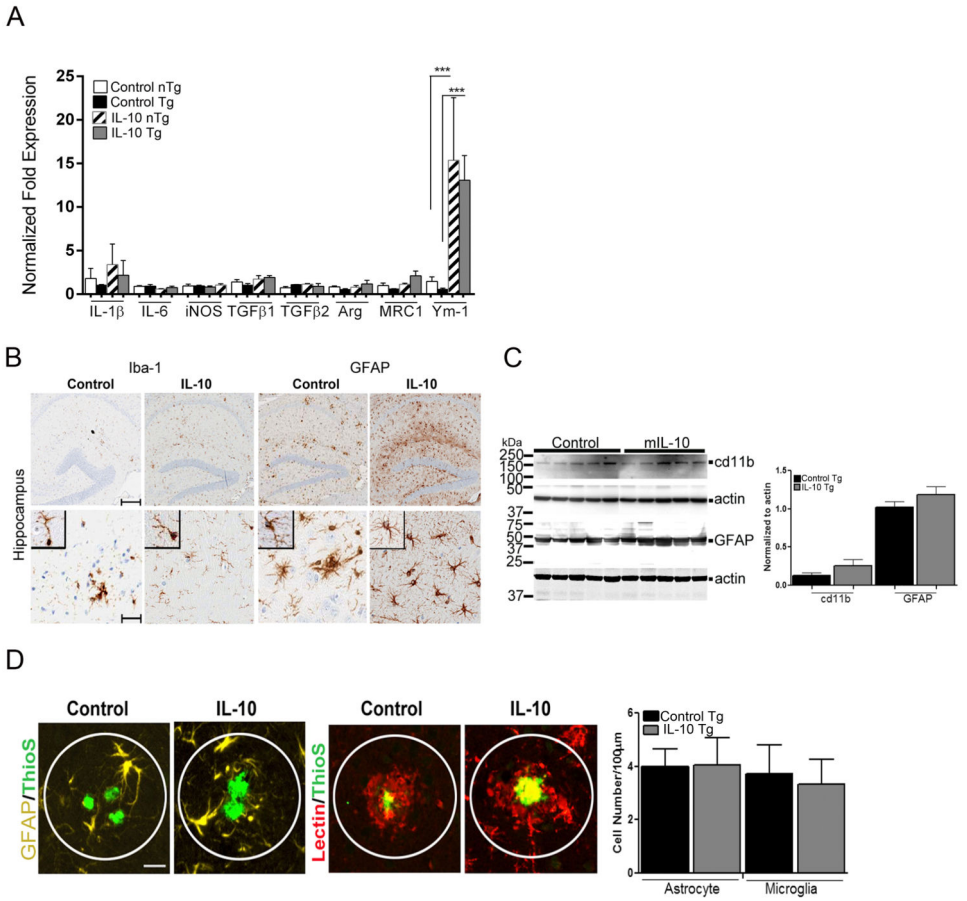

Figure 5. IL-10 expression leads to an M2 phenotype and does not affect astrogliosis or plaque engagement of astroglia in TgCRND8 mice

A. Sustained IL-10 production leads to a partial M2 phenotype in 6 month Tg and nTg littermate brains in CRND8 mice. Quantitative RT-PCR demonstrates that IL-10/Tg mice have elevated levels of M2 phenotype marker, Ym-1, but show no significant changes in MRC1 or Arginase (Arg). Analysis of three M1 phenotype markers, IL-6, iNOS or IL-1β, showed no changes. n=2-3 mice/group; each sample tested in triplicate. (***p<0.001, 1-way Anova with post-hoc Tukey's test).

B. Representative images of Iba-1 (microglia) and GFAP (astrocyte) immunoreactivity in intact hippocampus (top) and higher magnification of selected area of interest (bottom) from Control/Tg and IL-10/Tg mice is shown. Insets depict individual cells (high magnification) from corresponding low magnification panels. Scale Bar, 125μm (top), 25μm (bottom), 12.5 μm (insets, bottom). n=6mice/group.

C. Representative immunoblot and densitometric analysis of normalized levels of GFAP and cd11b obtained from 6 month old IL-10/Tg and Control/Tg mice. Molecular weight markers are indicated on the left (kDa). The lower panels represent blots re-probed with anti-actin antibody to depict loading amount. n=5 mice/group; p>0.05, 1-way Anova with Tukey's multiple comparison test. Data represents mean ± sem.

D. IL-10 expression does not alter astrocytic or microglial engagement around cored Aβ plaques. The number of astrocytes (GFAP-Cy3) and microglia (Dylight 594 conjugated

Tomato Lectin) engaged closely with the ThioS reactive plaques were quantified by counting the number of DAPI positive nuclei (restricted by a circular area of 100μm diameter around each plaque core, as depicted by the white circle). Data represents mean ±sd. Scale bar, 25μm, n=6-7mice/group, 10 plaques/mouse. See also Figure S5.

A

	Treatment					
	IL-10		Aβ42		IL-10+Aβ42	
NanoString Name	Log ratio	P-Value	Log ratio	P-Value	Log ratio	P-Value
C1qa	0.65	0.00	0.68	0.00	0.55	3.34116E-34
C1qb	0.47	0.00	0.40	0.00	0.21	0.00
C3	-0.77	ns	5.20	0.00	3.34	0.00
C3ar1	-0.17	1.65483E-34	0.42	0.00	-0.73	0.00
Ccl2	-0.31	ns	2.79	5.7881E-13	3.26	9.91921E-05
Ccl3	-0.39	0.00209147	1.47	9.0644E-35	-0.10	0.00
Ccl4	0.06	ns	0.89	ns	-0.22	0.00265145
Ccl5	-1.87	ns	5.28	0	4.00	0.00
Ccl8	0.71	ns	0.39	ns	3.16	2.75872E-06
Cd40	0.51	ns	4.18	1.1715E-07	2.91	0.000672418
Cdc42	-0.17	4.06452E-31	-0.02	9.6873E-07	-0.23	5.51847E-08
Cebpb	0.79	6.67427E-17	0.62	0.00036103	1.66	3.09435E-23
Cxcl10	-0.19	ns	5.19	9.379E-26	2.78	5.04839E-19
Cxcr4	0.05	ns	-3.36	1.8068E-23	-2.58	ns
Ddit3	-0.62	0.00122405	0.61	0.00426164	-0.31	2.69588E-05
Ifitm3	0.00	ns	-0.43	2.832TE-05	-0.70	ns
Il1b	1.16	ns	2.22	0.0006917	3.18	0.00020436
Stat1	-0.70	ns	2.56	0.00	1.81	3.32008E-17
Tgfb1	-0.08	ns	0.57	8.2286E-08	0.20	6.79825E-06
Thr1	0.28	ns	3.62	1.5105E-17	2.54	3.59364E-07
Thr2	0.25	ns	1.93	8.8604E-05	2.10	ns
Tnf	-0.02	ns	3.59	3.7067E-09	2.12	7.66798E-06

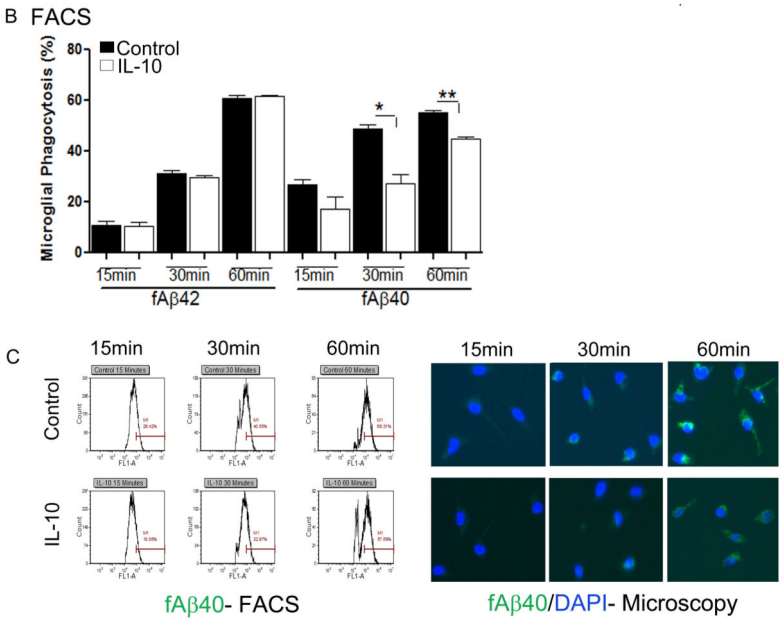

Figure 6. Recombinant IL-10 attenuates fAβ40 uptake by primary glia

A. List representing log ratio changes of differentially expressing genes in primary murine microglia treated with 10μM fAβ42 or IL-10, alone or in combination, following analysis by NanoString Inflammation GX array (q=0.05). n=3/group. A selected set of altered transcripts is shown as fold ratio change over naïve glia. n=2-3/treatment.

B. IL-10 treatment decreases microglial phagocytosis of fAβ40 but does not affect fβ42 uptake. Flow cytometric analysis for the presence of Aβ42-Hilyte555 or Aβ40-Hilyte488 in primary mouse glia cells was done following exposure to Aβ or vehicle control for various times (15 minutes to 1 hour). Data represents percent of microglial population positive for 555nm or 488nm fluorescence (mean±sem). (*p<0.05, **p<0.01, unpaired 2-tailed t test).

C. Representative pictograms depicting flow cytometric (FACS) and microscopic analysis of IL-10 or vehicle (Control) treated primary microglia internalizing fAβ40-488nm at different timepoints. See also Figure S6.

A

NanoString Name	Log ratio	P-value
Ccl8	6.25	2E-18
H2-Ea	5.21	2E-05
H2-Eb1	3.66	0.0002
C4a	2.37	0.00
C1qb	1.47	0.00
C1qa	1.44	0.00
Cdc42	-0.11	8E-12
Map2k1	-0.18	2E-12
Gnb1	-0.20	3E-18
Rac1	-0.21	2E-09
Atf2	-0.23	9E-08
Rapgef2	-0.23	0.001
Map2k4	-0.24	0.0002
Gnas	-0.26	0.00
Mef2c	-0.29	3E-05
Gnaq	-0.31	0.0006
Mapk8	-0.34	3E-05
Prkca	-0.47	7E-10
Nr3c1	-0.49	1E-06
Prkcb1	-0.54	0.00
Plcb1	-0.65	9E-32

B

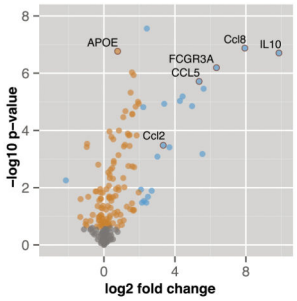

C

Accession	NanoString Name	IPA Name	Log ratio	P-value	Q-value
NM_011413.2	c4a	C4A/C4B	2.4187	2.75E-08	7.93E-07
NM_010548.1	IL-10	IL10	9.8607	1.98E-07	1.42E-06
NM_021443.2	Ccl8	Ccl8	7.9403	1.33E-07	1.43E-06
NM_009696.2	ApoE4	APOE	0.775	1.73E-07	1.43E-06
NM_144559.1	FcγRIV	FCGR3A	6.3431	6.43E-07	3.71E-06
NM_009779.2	C3ar1	C3AR1	1.5805	9.37E-07	4.50E-06
NM_009777.2	C1qb	C1QB	1.6722	1.17E-06	4.81E-06
NM_013653.3	CCL5	CCL5	5.3601	1.94E-06	6.99E-06
NM_010382.2	H2-Eb1	HLA-DRB1	5.6153	3.53E-06	1.13E-05
NM_007572.2	C1qa	C1QA	1.5037	4.76E-06	1.37E-05

D

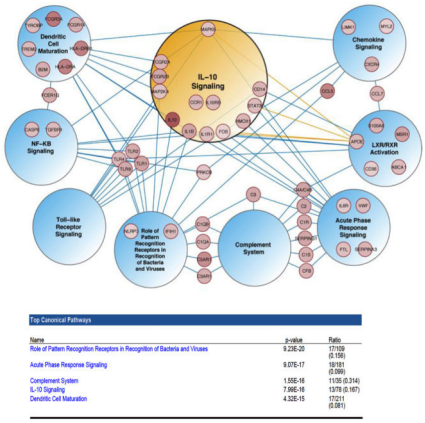

Top Canonical Pathways

Name	p-value	Ratio
Role of Pattern Recognition Receptors in Recognition of Bacteria and Viruses	9.23E-20	17/109 (0.156)
Acute Phase Response Signaling	9.07E-17	18/181 (0.099)
Complement System	1.55E-16	11/35 (0.314)
IL-10 Signaling	7.99E-16	13/78 (0.167)
Dendritic Cell Maturation	4.32E-15	17/211 (0.081)

E

Network name	# of genes	P-value	Q-value
Crosstalk between Dendritic Cells and Natural Killer Cells	14	0.0021645	0.0020297
FcγReceptor-mediated Phagocytosis in Macrophages and Monocytes	7	0.0021645	0.0020297
NF-κB Signaling	22	0.0021645	0.0020297
Role of PKR in Interferon Induction and Antiviral Response	7	0.0021645	0.0020297
Protein Ubiquitination Pathway	5	0.0021645	0.0020297
Role of Macrophages, Fibroblasts and Endothelial Cells in Rheumatoid Arthritis	39	0.0021645	0.0020297
Regulation of the Epithelial-Mesenchymal Transition Pathway	12	0.0021645	0.0020297
Role of Osteoblasts, Osteoclasts and Chondrocytes in Rheumatoid Arthritis	25	0.0021645	0.0020297

Figure 7. Transcriptome profile of TgCRND8 mice in response to IL-10

A. List representing log ratio changes of differentially expressing genes in IL-10/Tg mice compared to Control/Tg mice as analyzed by NanoString Inflammation GX array (q=0.05). n=3/group.

B. Volcano plots highlighting differential expression of genes with IL-10 over-expression in IL-10/Tg compared to Control/Tg mice as analyzed by NanoString Neurodegeneration Custom Array. Orange circles indicate statistically significant changes with fold change <2 and blue circles represent fold changes > 2 ($q < 0.05$). n=6 mice/group. See Table S1, S2 for details.

C. Representative rank-ordered list of genes that are differentially upregulated in response to IL-10 expression in Tg mice. See Table S2 for details. $q<0.05$; n=6mice/group.

D. Network analysis of differentially expressed genes in TgCRND8 mice. All differentially expressed genes ($q < 0.05$) were submitted to IPA for canonical network analysis. Nine significant networks with known connections to AD are shown. Among the genes submitted (140 for *APP* mice), these 9 networks include 55 genes. Differentially expressed genes from the IL-10 network are all contained within the IL-10 sub-network circle. Blue edges connect genes to shared networks. Gold edges denote literature connections between ApoE and IL-10 canonical pathway genes. n=6 mice/group. See Table S4.

E. DIRAC output of rank-ordered network alterations in response to IL-10 signaling in *APP* mice. Table S5 describes detailed information of the genes in each network affected.

See also Figure S7, Tables S1-S5.

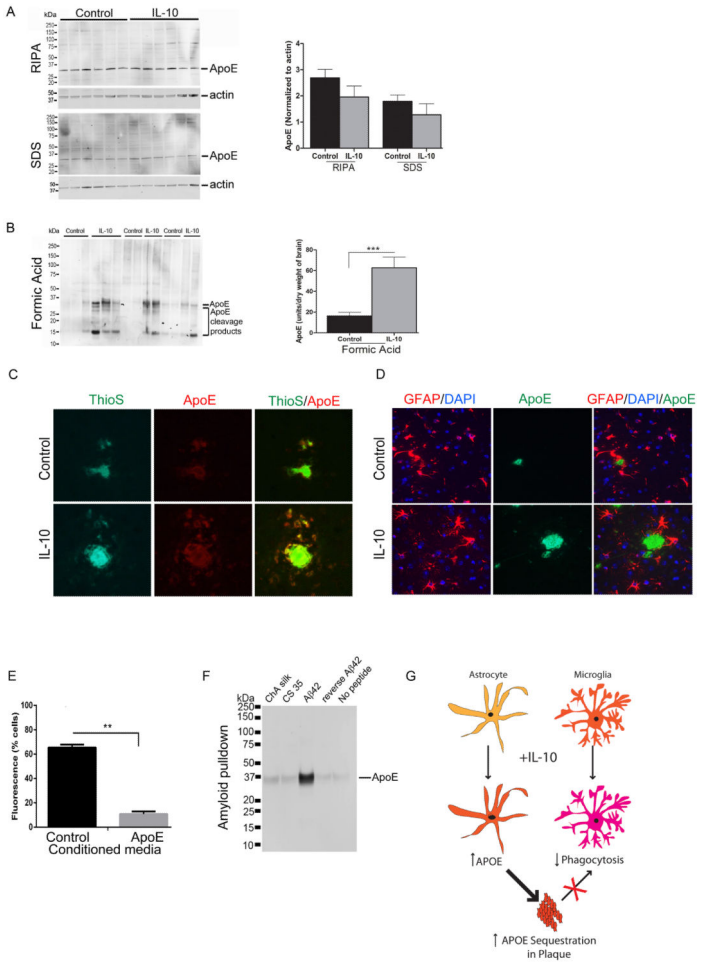

Figure 8. IL-10 induced ApoE is redistributed to insoluble plaque-associated cell fraction and impairs microglial uptake of Aβ

A-B. Representative anti ApoE immunoblots from sequentially extracted brain lysates-RIPA and SDS (A) and FA (B)- of TgCRND8 mice. Intensity analysis of immunoreactive bands of interest in the RIPA and SDS lysates were normalized to β-actin and that of FA lysates were normalized to dry weight of the hemibrain. Molecular weight markers are indicated (kDa). Data represents mean ± sem. n=6-7/group. ***p<0.001, 1-way Anova with Tukey's multiple comparison test.

C-D. Representative ThioS stained Aβ plaque shows increased plaque associated ApoE in IL-10/Tg mice cortex (C). Representative GFAP stained sections also demonstrate selective increase in plaque associated ApoE in IL-10/Tg mice (D). DAPI represents cellular nuclei. n=3-6/group.

E. Microglia grown in ApoE conditioned media internalize less fAβ40 compared to GFP conditioned media. Flow cytometric analysis for the presence of Aβ40-Hilyte555 was done following exposure to Aβ for 30 minutes. Representative data from two experiments is presented (**p<0.01, unpaired 2-tailed t test).

F. Amyloid pull down assay shows aggregated Aβ42 specifically binds ApoE in media. Representative assay from two independent experiments. ChA silk, silkmoth chorion 1-51 polypeptide; CS 35, bacterial cold shock polypeptide 1 -35.

G. Mechanistic insights into the pro-amyloidogenic effects of IL-10. IL-10 can directly dampen microglial phagocytosis; ApoE, induced by IL-10, may inhibit astroglial phagocytosis and removal of Aβ by binding to Aβ in plaques.
See also Figure S8.